euspen's 20th International Conference & Exhibition, Geneva, CH, June 2020
www.euspen.eu

Analysis of surface integrity of orthogonal diamond cut single-crystal Calcium Fluoride for ultraviolet and vacuum ultraviolet wavelength applications

Kai Rickens[1], Oltmann Riemer[1], Don A. Lucca[2]

[1] *Leibniz Institute of Materials Engineering IWT, Laboratory for Precision Machining (LFM), MAPEX Center for Materials and Processes, University of Bremen, Germany*
[2] *School of Mechanical and Aerospace Engineering, Oklahoma State University, Stillwater, OK 74078 USA*

rickens@iwt.uni-bremen.de

Abstract
Single-crystal calcium fluorite (CaF_2) is widely used for transmissive optics in ultraviolet and vacuum ultraviolet (UV and VUV) wavelength applications because of its exceptional transmission performance. Generally, products using CaF_2 are manufactured through finishing processes such as chemo-mechanical polishing (CMP), magnetorheological finishing (MRF) or ion-beam figuring (IBF) after performing precision cutting and grinding processes for profiling. However, CaF_2 is known as a brittle material with high anisotropy, and subsurface damage is induced by each cutting process. But, the effects of surface integrity on the optical and functional performance of precision machined CaF_2 has not been reported yet. In this research, a newly developed multiaxial adjustment system that can precisely align specimens is used in single-axis orthogonal cutting experiments with zero degree and negative rake angle diamond radius tools to prevent pre-machining and thus pre-damaging of single-crystal CaF_2 specimens. Cutting forces evaluation via piezoelectric dynamometer acquisition as well as surface analysis by atomic force microscopy and white light microscopy has been performed. Finally, smooth surfaces due to ductile material removal mechanisms could be determined on all machined specimen surfaces.

Single crystal calcium fluorite CaF_2, precision specimen alignment, ultra-precision diamond machining, surface and subsurface damage analysis

1. Introduction

Single crystal CaF_2 is one of only a few materials that can be used for transmissive optics in the vacuum ultraviolet (VUV) and ultraviolet (UV) wavelengths, but the mechanisms responsible for degradation of optical quality caused by machining processes are not scientifically understood [1]. This lack of understanding limits potential use in nanometer aspheric or free-form optics where diamond machining processes are used. Current studies are focused on machining of initial CaF_2 single crystal surfaces, damage-free polished by CMP and MRF, using a specially designed and analysed specimen alignment fixtures holding the work piece specimens [2]. The single crystal CaF_2 material having two different crystal orientations, (111) and (100) from two different manufacturers (A and B), were machined under a range of cutting conditions. The diamond cutting process and the generated surfaces have been characterized by cutting force measurement via piecoelectric dynamometer aquisition and a combination of atomic force microscopy (AFM) and white light interferometry (WLI).

2. Experimental procedure

Single crystal (111)CaF_2 from manufacturer A was used for initial cutting experiments on a 5-axis ultraprecison machine tool. Linear cutting, as illustrated in Fig. 1, was performed with a cutting direction of <101> and a cutting velocity of v_c = 50 mm/min. Single crystal diamond tools with a nose radius of r_ε = 1 mm were used and the nominal depth of cut was d_c = 3 µm. The diamond tools used have two different rake angles γ, 0° and -20°, and the feed step between each successive cut was either f = 10 or 15 µm, resulting in a total strip for surface and subsurface analysis of approx. b = 3 mm. Tip and tilt adjustment of the specimen were achieved by the developed alligment system to max. 70 nm deviation in X or Y direction of the machine tool to avoid pre-machining by face turning or milling and thus pre-damaging of the single crystal material.

The second set of specimens provided a much larger area for surface and sub-surface analysis, here b = 6 mm,. Single crystal (111)CaF_2 from manufacturer A was used again, as well as (111)CaF_2 and (100)CaF_2 from manufacturer B. The cutting direction for (111)CaF_2 was <101>, and <110> for (100)CaF_2.

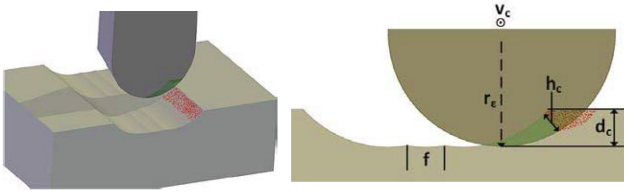

Figure 1. Schematic of cutting process with a round nose diamond tool.

The process parameters were again diamond tool nose radius r_ε = 1 mm, tool rake angles γ = 0° or -20°, cutting velocity v_c = 50 mm/min, and the step between each successive cut was reduced to f = 3 µm or 5 µm. Additionally, cutting forces were measured by a three-component piezoelectric dynamometer at a sampling rate of 10 kHz. The cutting force data was collected for the first 10 cuts, along with another two to four sets of 10 cuts during the subsequent machining process.

3. Results and discussion

Cutting forces

Figure 2 shows the cutting force F_c and thrust force F_p of the first 10 cuts in the (111)CaF_2 from manufacturer A cut with rake

angle γ = 0° and step of f = 3 µm. The cutting forces on the first cut are larger than the others since the diamond tool is fully engaged across its full width. Subsequent cuts have a smaller area of engagement with only the shoulder region of the diamond tool being enganged with the single-crystal material. Cutting forces from that point remain relatively constant. The sharp peaks in force signal observed between the cuts results from the stop and then backward motion of the y-axis and then positioning of the x-axis to position for the next cut.

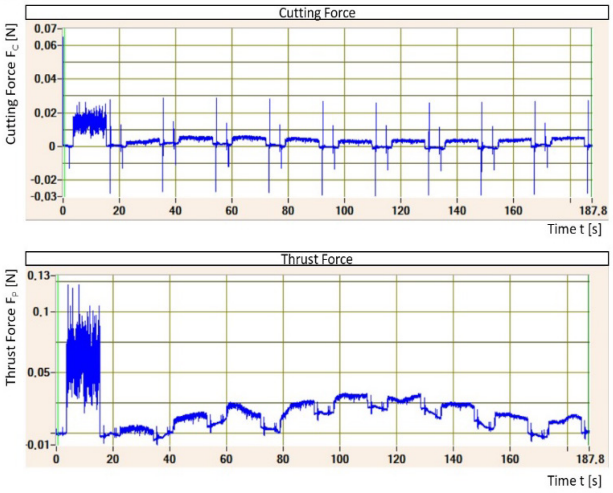

Figure 2. Cutting force F_c and thrust force F_p collected during the first 10 cuts of (111)CaF_2 from manufacturer A, γ = 0°, p = 3 µm.

Cutting forces for each specimen at various times during the cutting process are summarized in Table 1. The difference in cutting forces from a step f = 5 µm compared to 3 µm was relatively small. However, cutting forces for the specimens generated with γ = -20° were higher than those for specimens generated with γ = 0°. Cutting of (100)CaF_2 from manufacturer B resulted in much higher cutting and thrust forces in the first cut compared to all (111)CaF_2 specimens cut under the same parameters. After the initial cut forces were still higher for the (100)CaF_2, but only by a factor of approximately two.

Table 1. Summary of cutting forces collected at various times.

CaF_2 manufacturer and material type		A (111)	A (111)	A (111)	A (111)	B (111)	B (100)
Step f [µm]		5	3	5	3	5	5
Rake angle γ [°]		0	0	-20	-20	0	0
Cutting direction		<10$\bar{1}$>	<10$\bar{1}$>	<10$\bar{1}$>	<10$\bar{1}$>	<10$\bar{1}$>	<110>
First cut	F_c [mN]	14	20	92	110	10	480
	F_p [mN]	64	83	203	235	43	1059
	F_c/F_p ratio	0.22	0.24	0.45	0.47	0.23	0.45
Average of 9 cuts after the first	F_c [mN]	4	5	12	10	4	11
	F_p [mN]	10	7	20	17	9	22
	F_c/F_p ratio	0.40	0.71	0.6	0.59	0.44	0.50
Average of 10 cuts	F_c [mN]	6	7	15	15	5	12
	F_p [mN]	15	13	25	24	10	25
	F_c/F_p ratio	0.40	0.54	0.60	0.62	0.50	0.48

Surface analysis

AFM scans were performed on the machined CaF_2 over areas of 5x5 µm² and 20x20 µm² to investigate the surface topography and to measure the Ra surface roughness. Extensive pits and evidence of fracture was observed on all four of the machined surfaces. The Sa surface roughness as measured by AFM is shown in Table 2, as well as that measured by WLI. The surfaces machined with the higher step of f = 15 µm had higher surface roughness compared to those machined with the 10 µm step, which is consistent with the more extensive pits and fracturing that was observed from these surfaces.

Table 2 Surface roughness values from AFM and WLI analysis

Measured area/ magnification		Sa (nm)				
		AFM (20x20µm²)	AFM (5x5µm²)	WLI (5x mag.)	WLI (10x mag.)	WLI (20x mag.)
0° rake angle tool	10 µm step	34.0	33.5	30.2	33.3	50.4
	15 µm step	58.0	54.5	48.4	61.1	80.4
-20° rake angle tool	10 µm step	33.0	25.0	24.3	35.6	54.1
	15 µm step	55.5	45.0	50.9	68.0	92.4

AFM scans were performed on the CaF_2 over areas of 5x5 µm² and 20x20 µm² to investigate the surface topography and to measure the Sa surface roughness. Both of the surfaces machined from CaF_2 manufacturer B show more signs of pitting on the surfaces compared to those of manufacturer A.

The Sa values reported from the AFM measurements are the average of four scans, one from each quadrant of the specimen. In general, the surfaces generated with a 5 µm step had a slightly higher Sa than those created with f = 3 µm step. The (111)CaF_2 surface from manufacturer B had a Sa surface roughness that was two to three times that of the (111)CaF_2 from manufacuterer A, cut under identical process conditions.

4. Conclusion

Specimen alignment fixtures that were designed and built were used to diamond machine two sets of CaF_2 specimens for ultraviolet and vacuum ultraviolet (UV and VUV) wavelength experiments. Linear cutting of single crystal CaF_2 from two different manufacturers was performed with single crystal diamond tools with rake angle of either -20° or 0°.

Measured cutting forces show strong correlations to the applied tool rake angel and crystal orientation. Thus, higher cutting forces by larger negative rake angles and (100) oriented material compared to (111) materials.

The relatively high surface roughness Sa of the first set of (111)CaF_2 material, as measured by AFM, coincided with a decrease in transmittance compared to the initial material. The second set of specimens used (111)CaF_2 material from manufacturer A, as well as (111)CaF_2 and (100)CaF_2 from manufacturer B. Here, the surfaces generated with 3 µm steps had a slightly lower Sa than those created with 5 µm steps, resulting in an obviously higher surface integrity.

Acknowledgements

This work is supported by the German Research Foundation (DFG) under Grant No. RI 1108/9-1 and the US National Science Foundation (NSF) under Grant No. 1727244. We also acknowledge the kind support of Carl Zeiss Jena GmbH for providing materials.

References

[1] Wang, H., Riemer, O., Rickens, K., Brinskmeier, E.: "On the mechanism of asymmetric ductile-brittle transition microcutting of (111) CaF_2 single crystal". Scripta Materialia, 2016, Vol. 114, 21–26

[2] Shizuka, H., Rickens, K., Riemer, O. and Lucca, D.A.: "Development of a manual multi-axes workpiece adjustment system for ultraprecision diamond machining", Proc. 19th Int. euspen Conf., 2019, Vol. 3, 80-81.